

ON THERMOELECTRIC POWER IN n-CHANNEL INVERSION LAYERS ON
TETRAGONAL MATERIALS IN THE PRESENCE OF A PARALLEL
MAGNETIC FIELD

KAMAKHYA P. GHATAK, SANDIP BERA, ASHFAQUE ALI and BHASKAR NAG^a

*Department of Electronic Science, University of Calcutta, University College of Science
and Technology, 92, Acharya Prafulla Chandra Road, Calcutta 700009, India*

*^aDepartment of Applied Physics, University of Calcutta, University College of Science
and Technology, 92, Acharya Prafulla Chandra Road, Calcutta 700009, India*

Received 13 July 1995

UDC 538.93

PACS 72.15.Jf

We present a simplified analysis of thermoelectric power of carriers in n-channel inversion layers on tetragonal materials under the limits of weak and strong electric field, in the presence of a parallel magnetic field, at low temperatures. Taking n-channel inversion layers of CdGeAs₂ as an example, on the basis of a newly formulated 2D generalized electron energy spectra within the framework of $\vec{k}\vec{p}$ formalism incorporating various anisotropies of the energy band constants, it is found that thermoelectric power increases with decreasing surface electric field for both limits in oscillatory manners which are totally band structure dependent. The crystal field splitting reduces its numerical values. The thermopower exhibits oscillatory increment with increasing alloy composition for 2D system of ternary materials. The corresponding well-known results for the two-band Kane model in the absence of magnetic field have been obtained under certain limiting conditions as special cases of our generalized analysis.

1. Introduction

Thermoelectric power of electrons in semiconductors under magnetic field (TPM) is a very useful physical quantity, since the entropy (which can not be easily experimentally determined) can be derived from it when knowing experimental values of the electron concentration [1]. TPM is more accurate than any other relation for the entropy or the electron statistics, which are considered to be the two most widely used features of electron thermodynamics of quantum-confined materials. In recent years, with the advent of quantum Hall effect [2], there has been considerable interest in investigation of the TPM in various materials having different band structures at low temperatures where the quantum effects become prominent [3–6]. The analysis of the thermopower gives information about the band structure, the density-of-states function and the effective electron mass [7]. It appears that the TPM in n-channel inversion layers of tetragonal materials in the presence of a parallel magnetic field has yet to be understood for the more important case which occurs from the consideration of various types of anisotropies in the energy spectrum of these materials. This is very significant since the electron transport at low temperatures in 2D system in the presence of a parallel magnetic field has recently received considerable attention in the literature [8].

It may be stated that tetragonal materials, having strongly non-parabolic and non-standard energy bands, are increasingly used in Hall probes, thermal detectors [9] and light-emitting diodes [10]. Rowe and Shay [11] have demonstrated that the quasi-cubic model [12] can be used to explain the observed splitting and symmetry properties of both the conduction and valence bands at the zone center in \vec{k} -space of such compounds. The s-like conduction band is singly degenerate and p-like valence bands are triply degenerate. The latter splits into three sub-bands because of spin-orbit and crystal-field interactions. Kildal [13] proposed an electron dispersion law in the same material according to which the conduction band corresponds to a single ellipsoid of revolution at the zone-center in \vec{k} -space. He assumed an isotropic interband momentum matrix element and isotropic spin-orbit splitting of the valence band, although the anisotropies of the aforementioned band parameters are significant physical features of such compounds [14].

In Section 2.1 we shall study the TPM in n-channel inversion layers on tetragonal materials in the presence of a parallel magnetic field in limits of weak and strong electric field. We shall use the generalized Kildal model [15], by incorporating the anisotropies in the momentum matrix elements and the spin-orbit splitting parameters. In Section 2.2 we shall obtain the corresponding results for the three-band Kane model, the two-band Kane model and that of parabolic models in the presence of parallel magnetic field. In Section 2.3 we shall derive the well-known expressions of 2D dispersion relation, the density-of-states function, the 2D electron statistics in the absence of magnetic field and the TPM for the weak and strong electric field limits for n-channel inversion layers on small-gap materials whose energy band structures are defined by two-band Kane model which, in turn, will exhibit the indirect theoretical test of our generalized analysis. We shall plot the surface electric field dependence of the TPM under weak and strong electric field

limits taking n-channel inversion layers on CdGeAs₂ as an example. In addition, we shall also study the alloy composition dependence of the TPM for both limits, taking n-channel inversion layers on n-Hg_{1-x}Cd_xTe as an example.

2. Theoretical background

2.1. Formulation of TPM in n-channel inversion layers on tetragonal materials in the presence of a parallel magnetic field in accordance with the generalized band model for the weak and strong electric field limits

The generalized expression of the dispersion relation of conduction electrons in bulk specimens of tetragonal materials can be written as [15]

$$\rho(\varepsilon) = f_1(\varepsilon)p_s^2 + f_2(\varepsilon)p_z^2 \quad (1)$$

where

$$\rho(\varepsilon) = \varepsilon(\varepsilon + E_g) \left[(\varepsilon + E_g)(\varepsilon + E_g + \Delta_{||}) + \delta \left(\varepsilon + E_g + \frac{2}{3}\Delta_{||} \right) + \frac{2}{9}(\Delta_{||}^2 - \Delta_{\perp}^2) \right],$$

ε is the total electron energy as measured from the edge of the conduction band in the upward direction in the absence of any quantization, E_g is the band-gap, $\Delta_{||}$ and Δ_{\perp} are the spin-orbit splitting parameters parallel and perpendicular to the c -axis, respectively, δ is the crystal field splitting parameter, $p_s = \hbar k_s$, $\hbar = h/2\pi$, h is the Planck constant,

$$k_s^2 = k_x^2 + k_y^2,$$

$$f_1(\varepsilon) = \frac{E_g(E_g + \Delta_{\perp})}{2m_{\perp}^*(E_g + 2\Delta_{\perp}/3)} \left[\delta \left(\varepsilon + E_g + \frac{1}{3}\Delta_{||} \right) + (\varepsilon + E_g) \left(\varepsilon + E_g + \frac{2}{3}\Delta_{||} \right) + \frac{1}{9}(\Delta_{||}^2 - \Delta_{\perp}^2) \right],$$

$$f_2(\varepsilon) = \frac{E_g(E_g + \Delta_{||})}{2m_{||}^*(E_g + 2\Delta_{||}/3)} \left[(\varepsilon + E_g) \left(\varepsilon + E_g + \frac{2}{3}\Delta_{||} \right) \right],$$

and $m_{||}^*$ and m_{\perp}^* are effective electron masses at the edge of the conduction band, parallel and perpendicular to the direction of c -axis, respectively. Thus, extending the method as given in Ref. 16, the 2D electron dispersion laws in n-channel inversion layers of tetragonal materials in the presence of a parallel magnetic field

B along y direction can, respectively, be written under weak and strong electric field limits, as

$$\rho(E) = w_1(E, i)p_s^2 + w_2(E, i)p_x + w_3(E, i) \quad (2a)$$

and

$$\rho(E) = X(E, i)p_s^2 + Y(E, i)p_x + Z(E, i) \quad (2b)$$

where E is the total electron energy in the upward direction as measured from the edge of the conduction band at the surface,

$$w_1(E, i) = f_1(E) + \frac{2}{3}S_i(\hbar eF_s)^{2/3}(f_2(E))^{1/3}.$$

$$\cdot (f_2'(E) - f_1'(E)) \left[(\rho'(E)) - \frac{f_2'(E)\rho(E)}{f_1(E)} \right]^{-1/3},$$

S_i are the zeros of the Airy function [17], F_s is the normal surface electric field along z -direction, i is the electric sub-band index ($i = 0, 1, 2, \dots$), e is the electron charge, the single prime denotes single differentiation with respect to E ,

$$w_2(E, i) = \frac{4S_i B f_1(E)}{3F_s} (\hbar^2 e^2 F_s^2 f_2(E))^{1/3} [(\rho'(E) - f_2'(E)\rho(E)(f_1(E))^{-1})^{-1/3}],$$

$$w_3(E, i) = S_i (\hbar^2 e^2 F_s^2) (f_2(E))^{1/3} \left[\rho'(E) - \frac{f_2'(E)\rho(E)}{f_1(E)} \right]^{2/3},$$

$$p_x = \hbar k_x,$$

$$X(E, i) = \left[f_1(E) + \frac{f_2(E)L(E, i)g_2(E)}{2\sqrt{g_1(E)}} \right],$$

$$L(E, i) = \frac{4}{3}\hbar e F_e (S_i)^{3/2} (f_2(E))^{-1/2},$$

$$g_2(E) = -\frac{1}{2}f''(E) + \frac{f_2''(E)f_1(E)}{2f_2(E)} + \frac{f_1''(E)f_2'(E)}{f_2(E)},$$

where the double prime denotes double differentiation with respect to E ,

$$g_1(E) = \frac{1}{2}\rho''(E) - \frac{B^2}{F_s^2}f_1(E) - \frac{f_2''(E)\rho(E)}{2f_2(E)} - \frac{f_2'(E)\rho'(E)}{f_2(E)},$$

$$Y(E, i) = \frac{z(E, i)g_3(E)}{2g_1(E)},$$

$$g_3(E) = \frac{2Bf_1'(E)}{F_s} - \frac{2f_2'(E)Bf_1(E)}{F_s f_2(E)}$$

and

$$z(E, i) = f_2(E)L(E, i)\sqrt{g_1(E)}.$$

The use of Eqs. (2a) and (2b) leads to the expressions for the density-of-states functions for weak and strong electric field limits as

$$N_w(E) = \frac{1}{8\pi\hbar^2} \sum_{i=0}^{i_{max}} K_1(E, i)H(E - E_w) \quad (3a)$$

and

$$N_s(E) = \frac{1}{8\pi\hbar^2} \sum_{i=0}^{i_{max}} K_2(E, i)H(E - E_s), \quad (3b)$$

respectively, where

$$K_1(E, i) = \frac{2w_2(E, i)w_2'(E, i) - 4w_1'(E, i)w_3(E, i) - 4w_1(E, i)w_3'(E, i)}{(w_1(E, i))^2} + \frac{4w_1(E, i)\rho(E, i) + 4w_1(E, i)\rho'(E, i)}{(w_1(E, i))^2} - 2 \frac{w_1'(E, i)(w_2^2(E, i) - 4w_1(E, i)w_3(E, i) - 4w_1(E, i)\rho(E, i))}{(w_1(E, i))^3}.$$

H is the Heaviside step function, E_w is the sub-band energy in the low electric field limit which can be obtained from the equation

$$\rho(E_w) - w_3(E_w, i) = 0, \quad (4a)$$

$$K_2(E, i) = \frac{2Y(E, i)Y'(E, i) - 4X'(E, i)Z(E, i) - 4X(E, i)Z'(E, i)}{(X(E, i))^2} + \frac{4\rho'(E, i)X(E, i) + 4\rho(E, i)X'(E, i)}{(X(E, i))^2} - 2 \frac{X'(E, i)(Y^2(E, i) - 4X(E, i)Z(E, i) + 4X(E, i)\rho(E, i))}{(X(E, i))^3},$$

E_s is the sub-band energy in the high electric field limit and can be obtained from the equation

$$\rho(E_s) - Z(E_s, i) = 0. \quad (4b)$$

Thus, combining Eqs. (3a) and (3b) with the Fermi–Dirac occupation probability factor, the electron concentration per unit area for both limits can, respectively, be expressed as

$$n_{ow} = (8\pi\hbar^2)^{-1} \sum_{i=0}^{i_{max}} (a_1(E_{Fw}, i) + a_2(E_{Fw}, i)), \quad (5a)$$

$$n_{os} = (8\pi\hbar^2)^{-1} \sum_{i=0}^{i_{max}} (a_3(E_{Fs}, i) + a_4(E_{Fs}, i)). \quad (5b)$$

E_{Fs} and E_{Fw} are the Fermi energies as measured from the edge of the conduction band at the surface in the absence of magnetic field in the upward direction for strong and weak magnetic field limits, respectively,

$$a_1(E_{Fw}, i) = \frac{2w_2^2(E, i) - 4w_1(E, i)w_3(E, i) + 4w_1(E, i)\rho(E, i)}{(w_1(E, i))^2} \Big|_{E=E_{Fw}},$$

$$a_2(E_{Fw}, i) = \sum_{r=1}^{S_0} \bar{\Delta}_{rw} (a_1(E_{Fw}, i)),$$

$$\bar{\Delta}_{rw,s} = 2(k_B T)^{2r} (1 - 2^{1-2r}) \zeta(2r) \frac{d^{2r}}{dE_{Fw,s}^{2r}},$$

k_B is the Boltzmann constant, T is the temperature, r is the set of real positive integers, $\zeta(2r)$ is the zeta-function of order $2r$ [17],

$$a_3(E_{Fs}, i) = \frac{Y^2(E_{Fs}, i) - 4X(E_{Fs}, i)Z(E_{Fs}, i) + 4\rho(E_{Fs}, i)X(E_{Fs}, i)}{(X(E_{Fs}, i))^2}$$

and

$$a_4(E_{Fs}, i) = \sum_{r=1}^{S_0} \bar{\Delta}_{rs} (a_3(E_{Fs}, i)).$$

The TPM for the present case can, in general, be expressed as [1]

$$G = \frac{X_0}{eN_0}, \quad (6a)$$

where X_0 and N_0 are the entropy and electron concentration per unit area when $i = 0$. Using the results of Tsidilkovskii [1], we get

$$G = \frac{\pi^2 k_B^2 T}{3eN_0} \frac{\partial N_0}{\partial(E_F - E_0)} \quad (6b)$$

where E_F is the Fermi energy when $i = 0$ and E_0 is the zero-point energy.

Thus, combining the appropriate equations, the expressions of the TPM can easily be obtained for the weak and strong electric field limits.

2.2. Special cases

(a) Under the conditions $\delta = 0$, $m_{||}^* = m_{\perp}^* = m^*$ (isotropic effective electron mass) and $\Delta_{||} = \Delta_{\perp} = \Delta$ (the isotropic spin-orbit splitting parameter), Eq. (1) assumes the form

$$\frac{\hbar^2 k^2}{2m^*} = G(\varepsilon),$$

$$G(\varepsilon) = \frac{(\varepsilon + E_g)(\varepsilon + E_g + \Delta)(E_g + 2\Delta/3)\varepsilon}{E_g(E_g + \Delta)(\varepsilon + E_g + 2\Delta/3)}, \quad (7)$$

which is known as the three-band Kane model [18]. Equation (7) is often used to study the electronic properties of III-V materials, in general, but should be used for n-InAs where $\Delta \approx E_g$. Besides, the electron energy spectra of ternary and quaternary alloys can also be described by Eq. (7). It may be noted that the III-V compounds find extensive applications as Bragg reflectors, distributed feedback lasers, passive filter devices, photo refractive materials and in integrated optoelectronics [19]. The ternary compounds are very important optoelectronics materials because their band-gap can be varied to cover the special range from 0.8 to 30 μm [20]. The material find extensive applications in infrared detectors and photovoltaic detector arrays [20]. The quaternary materials have also received considerable attention in heterojunction lasers, light emitting diodes, FETs and various optical devices. Besides, new types of integrated optical devices such as switches, modulators and filters are made from such quaternary systems [21].

Under the above mentioned substitutions, the 2D electron energy spectrum, the density-of-states function and the electron concentration in the presence of a parallel magnetic field in n-channel inversion layers on small-gap materials whose energy band structures are defined by three-band Kane model, for the weak and strong electric field limits can, respectively, be expressed as

$$G(E) = \frac{p_s^2}{2m^*} + \phi(E, i)P_x + \psi(E, i), \quad (8a)$$

$$G(E) = \frac{p_s^2}{2m^*} + Q(E, i), \quad (8b)$$

$$N_w(E) = \frac{m^*}{\pi\hbar^2} \sum_{i=0}^{i_{max}} [G'(E) - \psi'(E, i) + m^* \phi(E, i) \phi'(E, i)] H(E - E_w), \quad (9a)$$

$$N_s(E) = \frac{m^*}{\pi\hbar^2} \sum_{i=0}^{i_{max}} [G'(E) - Q'(E, i)] H(E - E_s), \quad (9b)$$

$$N_{ow}(E) = \frac{m^*}{\pi\hbar^2} \sum_{i=0}^{i_{max}} (a_5(E_{Fw}, i) + a_6(E_{Fw}, i)), \quad (10a)$$

$$N_{os}(E) = \frac{m^*}{\pi\hbar^2} \sum_{i=0}^{i_{max}} (a_7(E_{Fs}, i) + a_8(E_{Fs}, i)), \quad (10b)$$

where

$$\phi(E, i) = \frac{S_i}{m^*} (2eF_s m^* \hbar G'(E))^{2/3} \frac{B}{3m^* F_s G'(E)},$$

$$\psi(E, i) = \frac{S_i}{2m^*} (2eF_s m^* \hbar G'(E))^{2/3},$$

$$Q(E, i) = \frac{2eF_s \hbar}{3m^*} (S_i)^{3/2} \sqrt{m^* G''(E)} \left[1 - \frac{B^2}{2m^* G''(E, i) F_s^2} \right].$$

E_w and E_s can, respectively, be determined from equations

$$G(E_w) - \psi(E_w, i) = 0 \quad (11a)$$

$$G(E_s) - Q(E_s, i) = 0 \quad (11b)$$

$$a_5(E_{Fw}, i) = m^* \phi^2(E_{Fw}, i) - 2\psi(E_{Fw}, i) + 2G(E_{Fw}),$$

$$a_6(E_{Fw}, i) = \sum_{r=1}^{S_0} \bar{\nabla}_{rw} (a_5(E_{Fw})), \quad a_7(E_{Fs}, i) = G(E_{Fs}) - Q(E_{Fs}),$$

$$a_8(E_{Fs}, i) = \sum_{r=1}^{S_0} \bar{\nabla}_{rw} (a_7(E_{Fs}, i)).$$

Thus, combining the appropriate equations with Eq. (6b), the expressions for the TPM for the weak and strong electric field limits can easily be obtained in this case.

(b) For $\Delta \gg E_g$ or $\Delta \ll E_g$, Eq. (7) is simplified:

$$\varepsilon(1 + \alpha\varepsilon) = \frac{\hbar^2 k^2}{2m^*}, \quad \alpha = \frac{1}{E_g}. \quad (12)$$

Equation (12) is known in the literature as the two-band Kane model [22]. In this case the basic forms of (8) to (11) will be unaltered where

$$G(\varepsilon) = \varepsilon(1 + \alpha\varepsilon), \quad G'(\varepsilon) = (1 + 2\alpha\varepsilon), \quad G''(\varepsilon) = 2\alpha.$$

(c) For parabolic energy bands, $E_g \rightarrow \infty$, Eq. (12) assumes the well-known form

$$\frac{\hbar^2 k^2}{2m^*} = \varepsilon. \quad (13)$$

In this case, the basic forms of Eqs. (8a), (9a), (10a) and (11a) will be unaltered where $G(\varepsilon) = \varepsilon$, $G'(\varepsilon) = 1$ and $G''(\varepsilon) = 0$.

2.3. Simplified results for the two-band models of Kane in the absence of magnetic field

Under the conditions $\Delta > E_g$, $\Delta \ll E_g$, $B \rightarrow 0$, $S_i^{3/2} \rightarrow (3/2)(i + 3/4)$ [17], $\alpha E_w \ll 1$ and $\alpha E_s \gg 1$, the expressions for the 2D electron dispersion law, the density-of-states function and the surface electron concentration for the two-band Kane model in the absence of magnetic field for the weak and strong electric field limits can, respectively, be expressed as

$$E(1 + \alpha E) = \frac{\hbar^2 k_s^2}{2m^*} + \left[\frac{3\pi e F_s \hbar (1 + 2\alpha E)}{2\sqrt{2m^*}} \right]^{2/3} \left(i + \frac{3}{4} \right)^{2/3}, \quad (14a)$$

$$E(1 + \alpha E) = \frac{\hbar^2 k_s^2}{2m^*} + \frac{2\pi e F_s \hbar}{\sqrt{2m^* E_g}} \left(i + \frac{3}{4} \right)^{2/3}, \quad (14b)$$

$$N_w(E) = \frac{m^*}{\pi \hbar^2} \sum_{i=0}^{i_{max}} (C_1 + C_2 E) H(E - E_w), \quad (15a)$$

$$N_s(E) = \frac{m^*}{\pi \hbar^2} \sum_{i=0}^{i_{max}} (1 + 2\alpha E) H(E - E_s), \quad (15b)$$

$$n_{ow} = \frac{m^* k_B T}{\pi \hbar^2} \sum_{i=0}^{i_{max}} (C_1 F_0(\eta_1) + C_2 k_B T F_1(\eta_1) + C_2 E_w F_0(\eta_1)), \quad (16a)$$

$$n_{os} = \frac{m^* k_B T}{\pi \hbar^2} \sum_{i=0}^{i_{max}} ((1 + 2\alpha E_s) F_0(\eta_2) + 2\alpha k_B T F_1(\eta_2)), \quad (16b)$$

where

$$E_w = \frac{1}{2\alpha} \left[- \left(1 + \frac{\alpha \bar{S}_i}{3m^*} (2eF_s \hbar m^*)^{2/3} \right) + \sqrt{\left(1 + \frac{\bar{S}_i}{3m^*} (2eF_s \hbar m^*)^{2/3} \right)^2 + \frac{2\alpha^2 \bar{S}_i}{m^*} (2eF_s \hbar m^*)^{2/3}} \right],$$

$$\bar{S}_i = \left[\frac{3}{2} \left(i + \frac{3}{4} \right) \right]^{3/2},$$

$$E_s = \frac{1}{2\alpha} \left[-1 + \sqrt{4\alpha(2\hbar e F_s / 3m^*)(S_i)^{2/3}(2\alpha m^*)^{1/2} + 1} \right],$$

$$\eta_1 = \frac{E_{Fw} - E_w}{k_B T},$$

$$\eta_2 = \frac{E_{Fs} - E_s}{k_B T},$$

$$C_1 = 1 - \frac{2\alpha \bar{S}_i}{3m^*} (2eF_s \hbar m^*)^{2/3},$$

$$C_2 = 2\alpha \left(1 + \frac{2\alpha E_{Fw}}{9m^*} (2eF_s \hbar m^*)^{2/3} \right),$$

and $F_j(\eta)$ is the one-parameter Fermi-Dirac integral of order j [23]. It must be mentioned that Eqs. (14a) and (14b) describing the 2D electron energy spectra of n-channel inversion layers on small-gap materials, whose energy band structures are defined by the two-band Kane model, was derived for the first time by AntocliFFE et al. [24]. The corresponding electron statistics as given by Eqs. (16a) and (16b) for the weak and strong electric field limits are also well-known in the literature [25].

We can summarize the theoretical background in the following way. We have formulated the expressions for the dispersion relation, the density-of-states function, the electron statistics and the TPM in n-channel inversion layers of tetragonal materials in the presence of the parallel magnetic field for the weak and strong electric field limits by considering the anisotropies of the momentum matrix elements and spin-orbit splitting parameters together with the proper consideration of

the anisotropic crystal potential in the Hamiltonian. We have simplified the above expressions for small-gap materials whose energy band structures are defined by the three-band Kane model and the two-band Kane model. We have also obtained the aforementioned expressions for the two-band Kane model in the absence of magnetic field under certain limiting conditions which are well-known in the literature [24,25]. The above statement is the indirect theoretical test of our generalized analysis.

3. Results and discussion

Using the appropriate equations and taking the parameters [9] $m_{\perp}^* = 0.033m_0$, $m_{\parallel}^* = 0.037m_0$, $\delta = -0.21$ eV, $B = 1$ T, $E_g = 0.57$ eV, $\Delta_{\parallel} = 0.36$ eV, $\Delta_{\perp} = 0.30$ eV, $T = 4.2$ K and $\varepsilon_S = 14.3 \varepsilon_0$, we have plotted the normalized TPM versus electric

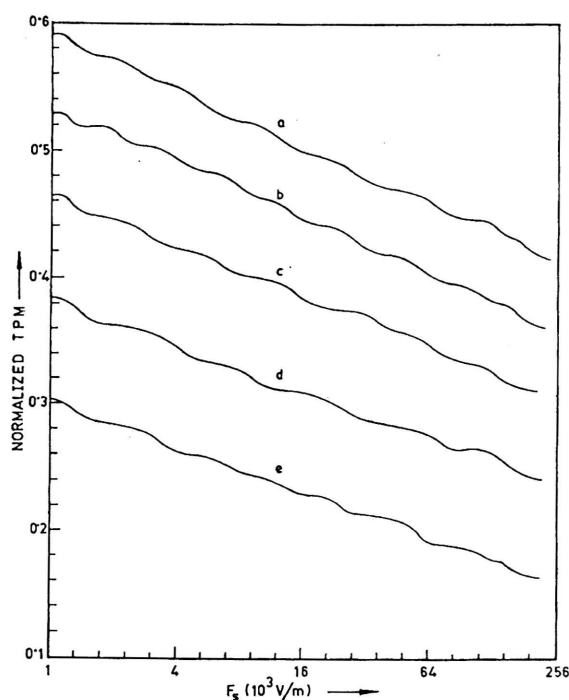


Fig. 1. Plots of the normalized TPM versus F_s in the low electric field limit in n -channel inversion layers of CdGeAs_2 in the presence of parallel magnetic field for (a) our proposed band model, (b) $\delta = 0$; (c) three-band Kane model, (d) two-band Kane model and (e) parabolic energy band.

field limits in n -channel inversion layers on CdGeAs_2 in the presence of a parallel magnetic field (Figs. 1 and 2, respectively). The curve b corresponds to $\delta = 0$; it

has been plotted for the purpose of assessing the influence of crystal field splitting on the TPM. Using the appropriate equations, the plots of TPM corresponding to the three-band Kane model, two-band Kane model and that of parabolic bands of n-channel inversion layers on CdGeAs₂, with an effective electron mass $m^* = 0.035m_0$ and $\Delta = 0.35$ eV (for the purpose of numerical computations of the three-band Kane model), are also shown in Figs. 1 and 2 for the weak and strong electric field limits, respectively. Using the appropriate equations and the parameters [19] $\Delta = (0.63 + 0.24x + 0.27x^2)$ eV, $E_g = (-0.302 + 1.93x + 5.25 \times 10^{-4} T(1 - 2x) - 0.810x^2 + 0.832x^3)$ eV, $m^* = 3\hbar E_g/4p^2$, $p^2 = (\hbar^2/2m_0)(18 + 3x)$ and $T = 4.2$ K for n-Hg_{1-x}Cd_xTe, we have plotted the normalized TPM versus the alloy composition (shown in Figs. 3 and 4) for the parabolic, two-band and three-band Kane models for the high and low electric field limits, respectively.

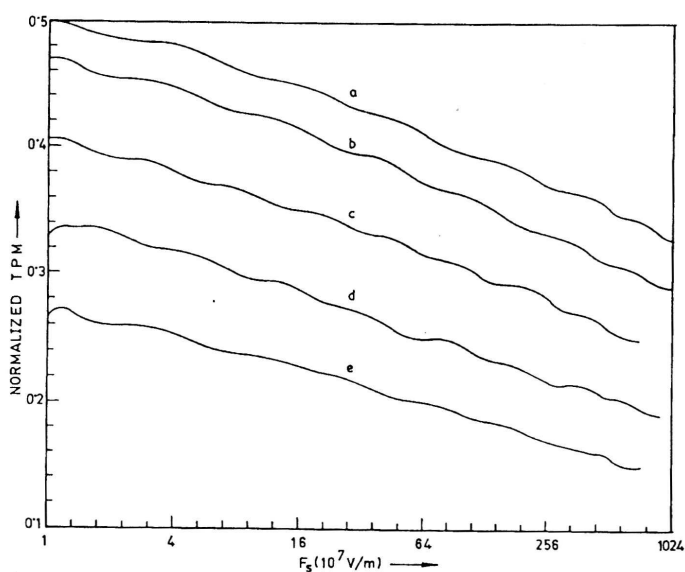


Fig. 2. Plots of the normalized TPM (for $B = 2$ T) in the high electric field limit in n-channel inversion layers of CdGeAs₂ in the presence of parallel magnetic field for all cases of Fig. 1.

From Figs. 1 and 2, it appears that the TPM increases in an oscillatory way with decreasing surface electric fields for both limits. The crystal field splitting parameter diminishes the numerical values of the TPM as evident from both figures. The TPMs corresponding to different dispersion laws differ widely in accordance with various band models. The TPM increases with increasing alloy composition in oscillatory manner for both limits which is also apparent from Figs. 3 and 4.

From the figures, it appears that the crystal field affects the TPM quite significantly in n-channel inversion layers of tetragonal materials for both limits under parallel magnetic field. Though TPM also increases nonlinearly with decreasing surface fields for both limits in various other limiting cases, the rates of increase

are different from that in the proposed band model. It may also be noted that if the direction of application of surface electric field applied perpendicular to the surface is taken as one of the transverse directions and not as a longitudinal one as assumed in the present work, the TPM would be different analytically for both limits. Nevertheless, the arbitrary choice of the direction normal to the surface would not result in a change of the basic qualitative features of TPM in the present case. The plots for n-channel inversion layers of ternary materials are valid for $x > 0.17$, since for $x < 0.17$, the band-gap becomes negative in $\text{Hg}_{1-x}\text{Cd}_x\text{Te}$, leading to the semi-metallic state, although our analysis is valid for n-channel inversion layers of III-V semiconductors.

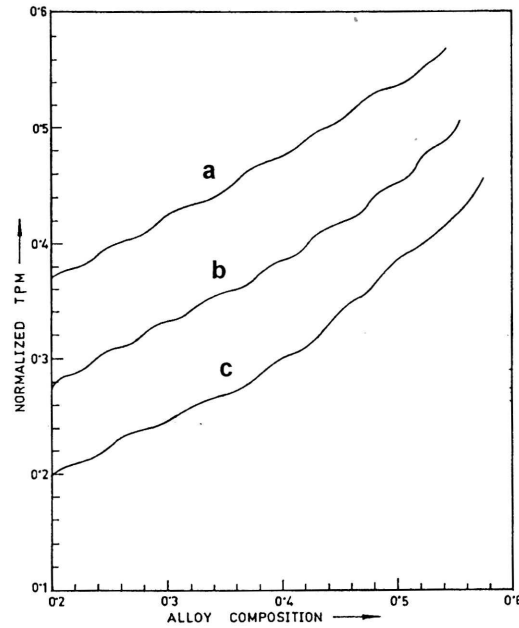


Fig. 3. Plots of the normalized TPM versus alloy composition (for $B = 1 \text{ T}$ and $F_s = 10^4 \text{ V/m}$) in the low electric field limit in n-channel inversion layers of $\text{Hg}_{1-x}\text{Cd}_x\text{Te}$ in the presence of parallel magnetic field (a) three-band Kane model; (b) two-band Kane model and (c) parabolic model.

It may be noted that the variations of the TPM are totally band structure dependent. The TPM could have been plotted for other physical variables. Our generalized formalism is valid for various types of 2D materials. We have plotted only the surface electric field and the alloy composition dependences of the TPM at both limits, considering only CdGeAs_2 and $\text{Hg}_{1-x}\text{Cd}_x\text{Te}$ in order to keep the presentation brief. Moreover, the general features of the effects of surface electric field and the alloy composition on the TPM as discussed here would be valid for most of the small-gap 2D materials having spherical constant energy surface, since our results are based on the generalized $\vec{k}\vec{p}$ formalism. The influence of energy band models on the TPM in the present case can also be assessed from our work.

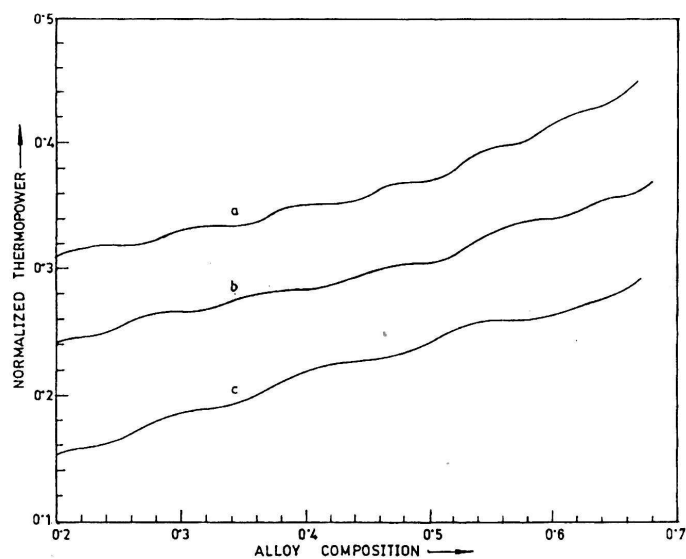


Fig. 4. Plots of the normalized TPM versus alloy composition (for $B = 2$ T and $F_s = 10^6$ V/m) in the high electric field limit for all cases of Fig. 3.

We wish to note that formulating the basic 2D dispersion relation, as given by Eqs. (2a) and (2b), we have considered the crystal field splitting parameter, the anisotropies of the momentum matrix elements and the spin-orbit splitting parameter. They are important physical features of tetragonal materials [15]. In the absence of crystal field splitting and with the assumptions of isotropic effective electron mass and isotropic spin-orbit splitting parameter, Eq. (1) converts into the three-band Kane model as given by Eq. (7). The three-band Kane model is valid for III-V compounds, ternary and quaternary alloys, but it should also be used for studying the physical properties of n-InAs where the spin-orbit splitting parameter is of the order of the band-gap. Incidentally, for many important small-gap materials, $\Delta \gg E_g$ or $\Delta \ll E_g$. Under these conditions, Eq. (7) converts into Eq. (12) which is known as the two-band Kane model. Finally, for $E_g \rightarrow \infty$, as for parabolic energy bands, Eq. (12) transforms into the well-known form $\varepsilon = \hbar^2 k^2 / 2m^*$. We have also obtained the well-known expressions of the 2D dispersion relation, the density-of-states function and the surface electron statistics for the weak and strong electric field limits in the absence of magnetic field for n-channel inversion layers on small-gap materials whose energy band structures are defined by the two-band Kane model which, in turn, presents the indirect theoretical tests of the TPM at low temperatures for the weak and strong electric field limits in n-channel inversion layers on small-gap materials having different band structures in the presence of a parallel magnetic field.

It may be remarked that only for materials having parabolic energy band we can obtain the exact 2D electron dispersion law for all values of surface electric field. However, the exact formulation of the same for the three-band Kane model, where

the combined influence of Δ and E_g have been taken into account, for all values of surface electric field without any approximation is not possible due to analytical difficulties [24]. In this paper, we have studied the TPM in n-channel inversion layers of tetragonal materials on the basis of the generalized $\vec{k}\vec{p}$ theory where the combined influence of the anisotropies in the effective electron mass and the spin-orbit splitting have been taken into account with the proper consideration of the crystal field splitting. Thus, the formulation of the exact 2D dispersion law for all values of the surface electric field presents a formidable problem. The formulation of any electronic property in any electronic material is based on the corresponding dispersion law. We have adjusted the physical parameters to obtain the inequalities in computations. It may be noted that the results for the low electric field limits can not be at all connected with the corresponding results of the high electric field limits, due to the presence of the fundamental defining inequalities for both the weak and strong electric fields regions, respectively.

We wish to note that since the experimental values of TPM in the present case are not available in the literature to the best of our knowledge, we can not compare our mathematical analysis with the experimental data, although the theoretical results as given in this context would be useful in analysing the experimental results when they appear. It may be noted that the present expressions of 2D electron statistics under parallel magneto-transport would be useful, since the study of the transport phenomena and the formulation of the various transport coefficients depend on the carrier statistics in such materials. Finally, we can write that the conclusions made here would be important in view of the fact that the Einstein relation for the diffusivity-mobility ratio, the electronic contribution to the elastic constants and the noise power can be connected with the TPM [26].

References

- 1) I. M. Tsidilkovskii, *Band Structures of Semiconductors*, (Pergamon Press, Oxford, 1982);
- 2) K. von Klitzing, *Rev. Mod. Phys.* **58** (1986) 519;
- 3) K. P. Ghatak, *Fizika A* **1** (1992) 207;
- 4) K. P. Ghatak and B. Mitra, *Nuovo Cimento* **15D** (1993) 97;
- 5) K. P. Ghatak and S. N. Biswas, *J. Appl. Phys.* **79** (1991) 4309;
- 6) K. P. Ghatak and M. Mondal, *Phys. Stat. Sol. (b)* **185** (1994) k5;
- 7) K. P. Ghatak, *Proc. of SPIE* **1584** (1992) 437;
- 8) R. A. Fisher, in *Non-Linear Optics Proc. of SPIE* **1594** (1992) 143;
- 9) S. I. Radautsan, E. A. Arushanov, A. P. Nateprov and G. P. Chuiko, *Cadmium Arsenide and Phosphide* (Nauka Press, Russia, 1976);
- 10) J. L. Shay, E. J. Beckmann, E. Bucher and J. H. Wernick, *Appl. Phys. Letts.* **23** (1973) 226;
- 11) J. W. Rowe and J. L. Shay, *Phys. Rev.* **83** (1971) 451;

- 12) J. J. Hopfield, J Phys. Chem. Solids **15** (1960) 97;
- 13) H. Kildal, Phys. Rev. **10B** (1974) 5082;
- 14) J. L. Shay and J. H. Wernick, *Ternary Chalcopyrite Semiconductors: Growth, Electronic Properties and Applications* (Pergamon Press, London, 1975);
- 15) K. P. Ghatak and M. Mondal, Fizika **18** (1986) 345;
- 16) F. Paasch, T. Fielder, M. Kolar and I. Bartos, Phys. Stat. Sol. B **118** (1983) 641;
- 17) M. Abramowitz and I. A. Stegun, *Handbook of Mathematical Functions* (Dover Publications, New York, 1965);
- 18) V. A. Vilkovskii, D. S. Domanevskii, R. A. Kakanov and V. V. Krasnovski, Sov. Phys. Semicond. **13** (1979) 553;
- 19) R. Dornhaus and S. Nimtz, Springer Tracts. in Mod. Phys. **78** (1976);
- 20) K. P. Ghatak and B. De, Proc. of MRS **234** (1991) 59;
- 21) K. P. Ghatak, M. Mondal and S. N. Biswas, J. Appl. Phys. **68** (1990) 3032;
- 22) B. R. Nag, *Electron Transport in Compound Semiconductors*, Springer Verlag, Berlin, Heidelberg, 1980;
- 23) K. P. Ghatak and S. N. Biswas, J. Wave Material Interaction **7** (1992) 171;
- 24) G. A. Antcliffe, R. A. Bates and R. A. Reynolds in *Proc. Internat. Conf. of the Physics of Semimetal and Narrow-Gap Semiconductors*, Edited by D. L. Carter and R. A. Bates (Pergamon Press, Oxford, 1971, p.506);
- 25) K. P. Ghatak and M. Mondal, J. Appl. Phys. **64** (1988) 918;
- 26) K. P. Ghatak, *Influence of Band Structures on Some Quantum Processes in Tetragonal Semiconductors*, D. Engg. Thesis, 1991, Jadavpur University, Jadavpur, India.

O TERMOELEKTRIČNOJ SNAZI U INVERZNYM SLOJEVIMA n-TIPA NA TETRAGONALNYM MATERIJALIMA U PARALELNOJ MAGNETSKOJ POLJU

Izlažemo pojednostavljenu analizu termoelektrične snage pokretnih nositelja naboja u inverznim slojevima n-tipa na tetragonalnim materijalima u granicama slabog i jakog električnog polja, u magnetskom polju i na niskim temperaturama. Na primjeru inverznih slojeva CdGeAs₂ n-tipa, na osnovi novih 2D generaliziranih elektronskih energijskih spektara i u okviru $\vec{k}\vec{p}$ formalizma uz različite anizotropije konstanta energijskih vrpce, utvrđeno je da termoelektrična snaga raste sa smanjenjem površinskog električnog polja na obje granice, uz oscilacije koje su potpuno ovisne o strukturi vrpce. Cijepanje kristalnog polja smanjuje termoelektričnu snagu. Termoelektrična snaga pokazuje oscilacijsko povećanje pri povećanom sastavu za 2D sisteme ternarnih materijala. Poznati rezultati dvo-vrpčastog Kaneovog modela se dobivaju uz neke granične uvjete kao posebni slučajevi naše općenite analize.